

Chitosan/PVA Nanofibers and Membranes: Preparation, Characterization, and Potential Applications

N.S. Yousef^{1,*}, F. Shokry², Mostafa Elkhatib³

¹ Petrochemicals Engineering Department, Faculty of Engineering, Pharos University, Alexandria, Egypt, email: noha.said@pua.edu.eg

² Chemical Engineering Department, Faculty of Engineering, Port Said University, Port Said, Egypt, email: fathi.shokry@eng.psu.edu.eg

³ Basic Engineering Department, Faculty of Engineering, Pharos University, Alexandria, Egypt, email: mostafa.elkhatib@pua.edu.eg

*Corresponding author, DOI: 10.21608/PSERJ.2023.228866.1255

ABSTRACT

Biopolymer chitosan has several desirable properties, including its abundance in nature, low cost, adaptable structure, diverse functional groups, high adsorption capacity, biocompatibility, and lack of environmental impact. It may be processed into many different forms, all of which exhibit numerous features linked to membranes, and ranks as the second most common biopolymer. Chitosan is made from recycled mussel shells. The study discussed here covers the development and characterization of fibers and adsorbent membranes based on a chitosan/polyvinyl alcohol (CS/PVA) blend for heavy metal removal and desalination. The resulting membrane was compared to a composite membrane formed by grafting PVA and Chitosan onto the CA-RO membrane. Two different membranes are compared to the Chitosan/Poly vinyl alcohol (CS/PVA) electrospun nano fibers that they create. Electrospinning was utilized to make nanofibers of CS/PVA. Two distinct types of Chitosan/PVA membrane were produced: one by blending chitosan and polyvinyl alcohol at a vol/vol ratio of 50/50, and the other by grafting PVA and Chitosan onto a CA-RO membrane. Heavy metal removal and desalination performance of both membranes were assessed. The crystallinity of the membrane and its structural properties was examined using scanning electron microscopy (SEM), X-ray powder diffraction (XRD), and infrared spectroscopy (FTIR). Electrospun fibers were found to be nanosized in scanning electron micrographs. Unlike the composite, which appeared smooth and homogenous in SEM micrographs, the CS/PVA membrane's surface is similar to that of fibers. When the composite membrane was cut in half, several grafted pores became visible. In the case of copper, chromium, and zinc ions, the CS/PVA membrane performed well for heavy metal removal. It also performed well in terms of salt removal. In both heavy metal and salt removal, however, composite membrane outperformed CS/PVA membrane.

Keywords: Chitosan fibers, Electrospinning, Chitosan/PVA membranes, Composite membranes, desalination, heavy metals.

Received 12-8-2023
Revised 15-10-2023
Accepted 5-11-2023

© 2023 by Author(s) and PSERJ.

This is an open access article licensed under the terms of the Creative Commons Attribution International License (CC BY 4.0).

<http://creativecommons.org/licenses/by/4.0/>



1 INTRODUCTION

Natural polysaccharides have long been used because to their exceptional biocompatibility and biodegradability [1]. Chitin is a naturally occurring polysaccharide that has outstanding bioactivities and is thought to be the second most common biopolymer

in nature [2]. It is mostly obtained from the exoskeletons of crustaceans, insects, and mollusks as well as the cell membranes of microorganisms [3]. Chitin may be challenging to extract since it is an insoluble biopolymer with a large molecular weight [4]. Additionally, chitosan is used in a variety of industries while using up to 15% less energy than other industrial materials [5–6]. There has been a

tremendous increase in research and development in the field of chitin/chitosan and its uses in recent years [4-8]. This promotes the development of novel products and the usage of chitin/chitosan in a wide range of industries [9]. Chitin/chitosan has been effectively used and employed in a variety of industries, including petrochemicals, pharmaceuticals, and nanotechnology [9]. Nanofibers offer incredible properties such as high surface area-to-volume ratio, good permeability, and extremely small hole sizes [10-11]. Chitosan-synthetic polymer blends are a feasible method for generating synthetic biodegradable polymers with different properties such as high- water absorbance and improved mechanical properties while keeping biodegradability [3]. Chitosan has also been combined with appropriate polymers such as cellulose acetate, acrylonitrile butadiene styrene, and polyvinyl alcohol to produce highly reactive and stable membranes [11]. The widespread usage of polyvinyl alcohol (PVA), a very hydrophilic and CS-compatible polymer, has improved the mechanical and chemical properties of chitosan membranes [5]. Aside from porosity and form, nanostructures can improve the sorption properties of chitosan membrane adsorbents [12]. Numerous molecules of matter have been electrically spun into nano scale fibres demonstrating the technique's efficiency in producing submicron-sized fibres. Surface charge is formed on a polymer fluid when a field of electricity is applied across the tip of the needle and the collecting surface, causing a sphere-shaped droplet to deform in a cone-like form. The provided fluid stream discharges as the field of electricity exceeds the repulsion caused by electrostatic force [13]. High concentration of electrical charges on the surface encourages the sprayed solution to break down creating a highly stretched polymeric fiber and the solvent evaporates quickly. Electrical voltage used, distance between tip and collector, input flow rate, and the properties of the polymer solution injected are all important electrospinning features [14]. This study has multiple objectives, including the following: Chitosan must first be made from mussel shells, then both CS and PVA fibers must be electrospun, followed by both CS and PVA membrane, and finally a composite membrane made by grafting PVA and Chitosan onto the CA-RO membrane (CS/PVA-CA-RO). Fourth, use rheological study of fibers and combine techniques like FTIR spectral analysis, scanning electron microscopy (SEM), and X-ray diffraction (XRD). Lastly, to examine the efficiency of both (CS/PVA) membrane and (CS/PVA- CA-RO) membranes in desalination and the removal of heavy metals.

2 MATERIALS AND METHODS

2.1 Materials

Mussel shells purchased from fish market. Acetic acid (glacial 100%, pro analyzed), Sodium hydroxide, Poly vinyl alcohol (PVA), Potassium persulphate, Copper salt, Chromium salt, and Zinc salt, all were purchased from El Gomhouria Company for Trading Chemicals and Medical Appliances, a local company in Egypt.

2.2 Preparation of Chitosan from Mussel Shells

In order to obtain chitin, mussel shells were procured at the fish market, cleaned, and dried. To make chitosan, mussels were soaked in a 40% concentrated NaOH solution for two hours at 60⁰ C, where the chitin in the mussels was deacetylated. After obtaining chitosan, it was cleaned with distilled water until it had a pH close to neutral (and was therefore devoid of alkali), and then it was allowed to dry overnight at room temperature. The chitosan was crushed and pulverized before being prepared for acetic acid dissolution.

2.3 Preparation of Chitosan/Poly (Vinyl Alcohol) fibers of electrospinning

Using a syringe pump, a commercially available syringe equipped with a steel needle was filled with chitosan-PVA solution at a rate of 0.8 mL per hour. This rate was maintained throughout the electrospinning procedure until a stable Taylor cone was obtained. The voltage DC generator was utilized to create voltage up to 22kV. To investigate the impact of voltage on the produced fibers, the voltage was changed to 28 kV. The cathode of the power supply was coupled to the collector, made up of a plate of copper wrapped in aluminium foil and situated 14 cm away from the tip of the needle. The power supply's anode was linked to the syringe's needle. The electrospun samples were stored in a silica gel-filled desiccator until analysis.

2.4 Preparation of Chitosan/Poly (Vinyl Alcohol) Blended Films

To create a 10 g L⁻¹ chitosan solution, five grammes of chitosan were mixed in 500 mL of 2% acetic acid, gently stirred, and heated at roughly 60⁰ C overnight. After that, the solution was filtered to get rid of any remaining dust and contaminants. To eliminate air bubbles, the solutions were kept at room temperature for two hours.

Same amount of PVA, 5 g, was dissolved in 500 mL of warmed, ultrapure water to create a 10 g L⁻¹ solution. After that, the mixture was mixed and held at roughly 800⁰ C for two hours.

A blended solution of chitosan-PVA (CS/PV) with a ratio of (50/50% vol) was formed by adding 35 ml of PVA solution drop by drop to 35 ml of chitosan solution, kept on a magnetic stirring device at about 94⁰ C and whirled at a moderate speed for 30 minutes. Homogeneous (CS/PVA) solution films were made by pouring specified amounts of the solution into polystyrene Petri plates and drying at 60⁰ C. The films were peeled off and stored in an evacuated desiccator.

2.5 Preparation of a composite of cellulose acetate-reverse osmosis (CA-RO) membrane and Chitosan-PVA (CS/PVA) solution

For five minutes, sodium hydroxide (0.04%) was applied to the top of the CA-RO membranes to partially deacetylate them. After thoroughly cleaning the membranes with deionized water, potassium persulfate (1.5 wt%) was applied drop-by-drop to the top surface of the CA-RO membrane for 10 minutes. For the grafting reaction to occur, PVA and Chitosan solution (50/50 % vol) were applied to the CA-RO membrane surface for 10 mins at room temperature. To get rid of unreacted compounds, deionized water was used to wash the functionalized CA-RO membranes several more times. The membranes were then thermally treated for 30 minutes at 75⁰ C.

1.1.1. Application of CS/PVA membrane and CA-RO/CS/PVA composite in heavy metal removal

Three separate heavy metal solutions (copper, chromium, and zinc) were created in 100 mL solutions with a concentration of 3 ppm each in order to test the constructed membranes' ability to adsorb the metals. Atomic absorption spectroscopy was used to determine the filtrate's residual concentration after the solution had passed through each membrane independently.

2.6 Application of CS/PVA membrane and CA-RO/CS/PVA composite in desalination

To examine both prepared membranes' capacity for desalination, A 156 g/L salt solution was made, and its conductivity was assessed both before and after membrane application.

3 RESULTS AND DISSUCTIONS

3.1 FTIR analysis of Chitosan-PVA membrane (50/50 % vol):

Figure 1 displays the FTIR spectra of the created Chitosan-PVA membrane (50/50 vol%). The figure shows the distinctive peaks of polymers at 1087cm⁻¹, 3309 cm⁻¹, and 2379 cm⁻¹ due to C-O stretch, N-H stretch, and C-H stretch, respectively, which validates the presence of both PVA and chitosan in the membrane [15]. In the range of 3300-3500 cm⁻¹, a prominent peak may be seen as one broad band and is attributable to the stretching vibration of O-H groups. The symmetric and asymmetric stretching vibration of C-H groups is related to the 2830-2930 cm⁻¹ peak. The stretching vibration of CO, which emerges with a wavelength of 1708 cm⁻¹, belongs to the carbonyl and carboxyl groups. Chitosan NH₂ and polyvinyl alcohol's OH group stretching vibrations are related to the wavelength of 3360 cm⁻¹. While the CO bonds of polyvinyl alcohol and chitosan and the CN bonds of chitosan are connected, the stretching vibration of CH appeared at 2935 cm⁻¹, and [16] at 1089 cm⁻¹.

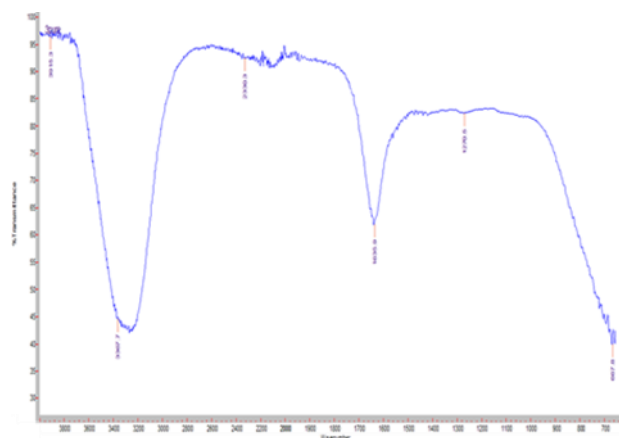


Figure 1: FTIR analysis of Chitosan-PVA membrane (50/50 vol%)

3.2 FTIR analysis of Chitosan-PVA pure solution (50/50 vol%):

The pure solution of chitosan-PVA (50/50 vol%) is analysed using FTIR in Figure 2. The stretching vibration of O-H groups is responsible for the strong peak that manifests as a single broad band in the range of 3300-3500 cm⁻¹; the stretching vibration of polyvinyl alcohol's OH group and chitosan's NH₂ are both related to the wavelength of 3360 cm⁻¹. The presence of both PVA and chitosan in the membrane can be seen by the distinctive polymer peaks at 1087 cm⁻¹, 3309 cm⁻¹, and 2379 cm⁻¹, which are caused, respectively, by C-O stretch, N-H stretch, and C-H stretch.

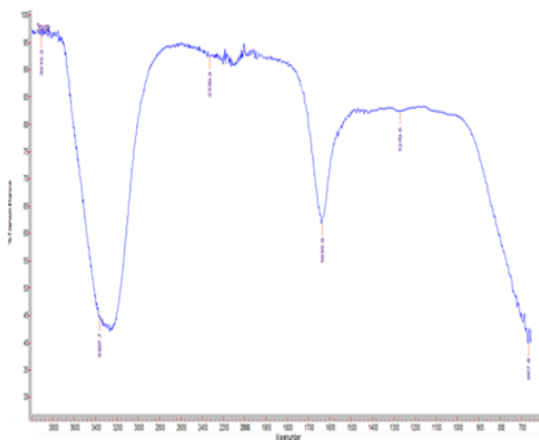


Figure 2: FTIR analysis of Chitosan-PVA pure solution (50/50 vol%)

3.3 FTIR analysis of CA-RO/CS/PVA composite membrane:

Figure 3 displays the FTIR spectra of the created CA-RO/CS/PVA composite membrane. The oxidation of the primary alcohols of native cellulose is confirmed by a prominent peak at 1734 cm⁻¹ that corresponds to the carbonyl group, as can be seen in the figure. The CS/PVA membrane does not exhibit this band.

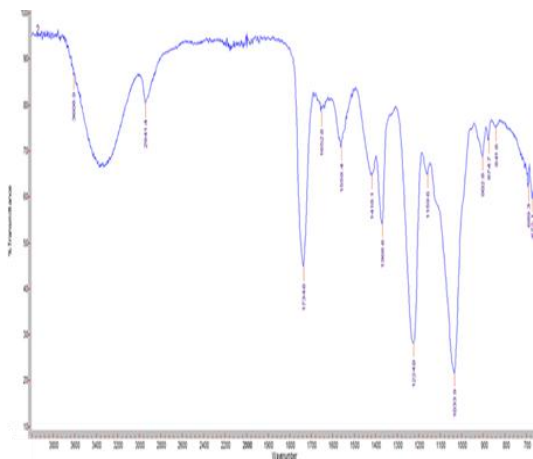


Figure 3: FTIR analysis of CA-RO/CS/PVA composite membrane

3.4 FTIR analysis of CA-RO membrane:

The FTIR spectra of the CA-RO membrane is shown in Figure 4. The figure displays three peaks. A strong peak in the O-H groups, with a range of 3300–3500 cm⁻¹

1, A peak corresponding to C=O between 1760 and 1690 cm⁻¹, followed by a peak for C=C at around 1600 cm⁻¹.

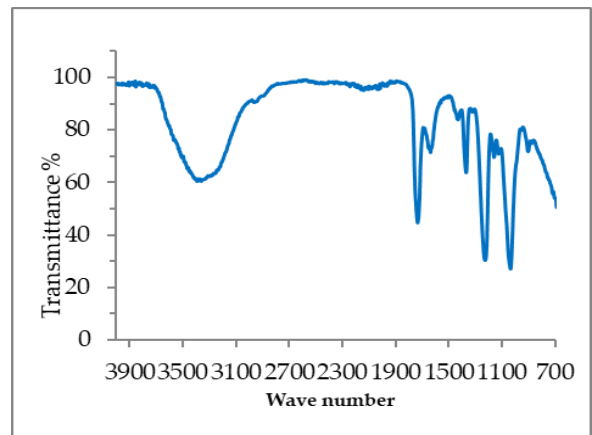


Figure 4: FTIR analysis of CA-RO membrane

3.5 SEM micrographs:

3.5.1 SEM micrographs of CS/PVA electrospun fibers:

Figure 5 depicts micrographs of CS/PVA electrospun fibers utilizing a 30/70 volume ratio of Chitosan-PVA solution in millimeters, a collector distance of 14 cm from the tip of the needle, a flow rate of 0.8 mL/hr using a syringe pump, and a voltage of 22 kV. The fibers are homogenous, with no thin or thick ones, and are in the nano range. These tests were carried out on aluminum foil.

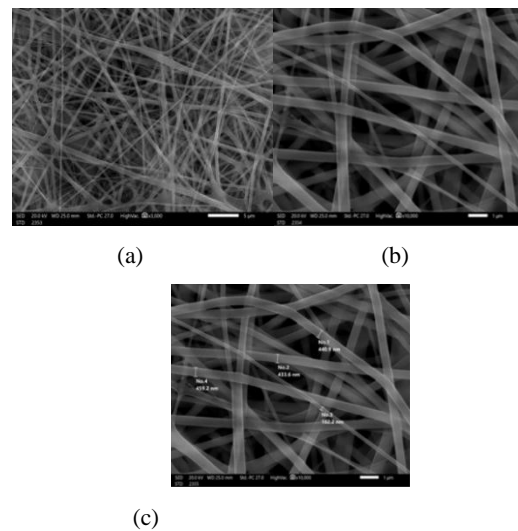
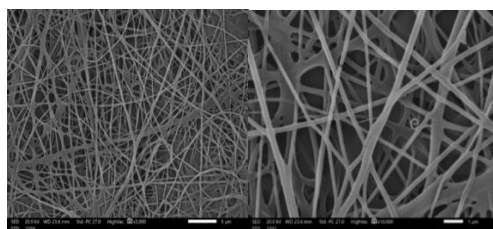


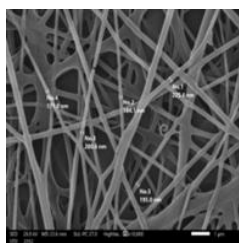
Figure 4: Micrographs of CS/PVA fibers (30/70) volume ratio with a voltage of 22k V, 14 cm collector distance, and a flow rate of 0.8 mL/h; a) at 5 μm, b) at 1 μm, and c) at 1 μm including diameters

Figure 6 depicts micrographs of CS/PVA electrospun fibers made using the same prior solution (30/70 volume ratio in millimetres), the same collector distance (14 cm from the tip of the needle), the same flow rate (0.8 mL/hr), and a different voltage of 28 kV instead of 22kV. The deposited fibers increased in size

as the electrospinning voltage increased; very few flaws and a relatively uniform morphology can be seen. In the case of high voltage, the fiber diameter is smaller than in the case of low voltage, and it is also smaller in the nano range.



(a) (b)

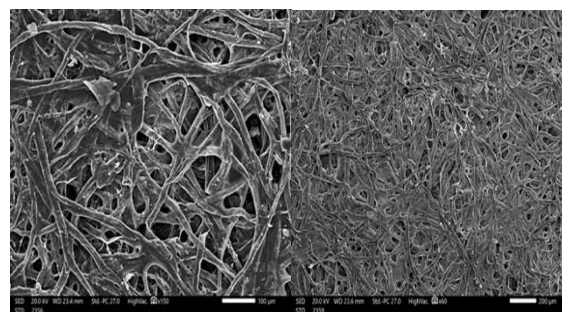


(c)

Figure 6: Micrographs of CS/PVA fibers (30/70) volume ratio with a voltage of 28 k V, 14 cm collector distance, and a flow rate of 0.8 mL/h; a) at 5 μm, b) at 1 μm, and at 1 μm including diameters

3.5.2 SEM micrographs of CS/PVA membranes (50/50 %vol):

The cross-section morphology and surface properties of membrane adsorbents are commonly studied using SEM [17]. Figures 7 and 8 display, for a sample containing CS/PVA (50/50 % vol), SEM images of the top surface and the cross-sectional area of the membrane, respectively. The micrograph of the membrane surface looks like that of the fiber, as can be observed in the pictures. The presence of hydrogen bonds between the functional groups of the blended component was the primary factor in the creation of CS and PVA fiber blends (–OH and –NH₂ groups in CS, and –OH groups in PVA).



(a) (b)

Figure 7: Micrographs of the surface of CS/PVA membranes (50/50 %vol); a) at 100 μm, b) at 200 μm

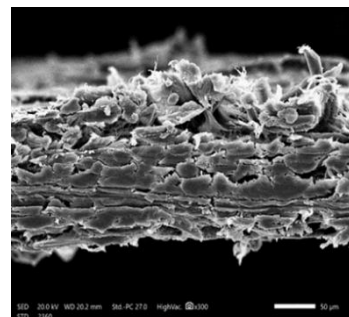
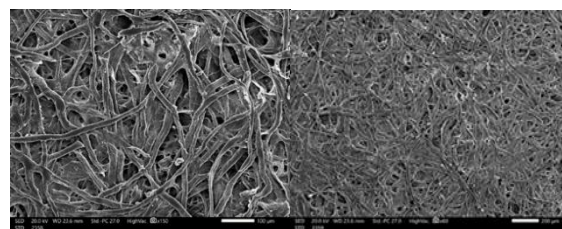


Figure 8: cross section of the CS/PVA membrane (50/50 %vol)

Figures 9.a and 9.b show the CS/PVA membrane's bottom surface at 100 and 200 micrometers, respectively. Figures depict how the membrane looks like fiber, complete with a formation of uniform CS and PVA blends.



(a) (b)

Figure 9: Micrographs of the bottom of CS/PVA membranes (50/50 %vol) at 100 μm; a) at 100 μm, b) 200 μm

3.5.3 SEM micrographs of CS/PVA membrane and CA-RO/CS/PVA composite membrane

To enable the grafting process, PVA and Chitosan solution (50/50 vol%) were applied to the CA-RO membrane surface. Figures 10, 11, and 12 depict, respectively, the composite membrane's surface, cross section, and bottom. It is obvious that the composite surface is uniform, smooth, and free of visible pores or

domains, as shown in Figure 10, demonstrating good compatibility between cellulose acetate and CS/PVA. Contrary to what is seen in the CS/PVA membrane, neither the bottom nor the surface appears to be made of fibers. Cross-sectional area of the composite as shown in Figure 11, demonstrates channels in the membrane that develop as a result of grafting CS/PVA membrane and CA-RO/CS/PVA membrane, which are not visible in CS/PVA membrane. There are several pores at the bottom of the membrane as shown in Figure 12, whereas there are none on the CS/PVA membrane.

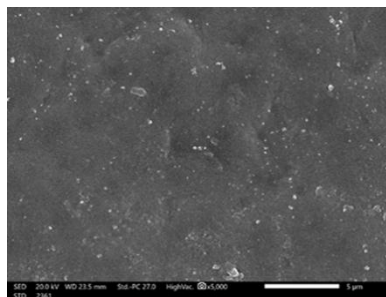


Figure 10: Micrographs of the surface of composite membrane

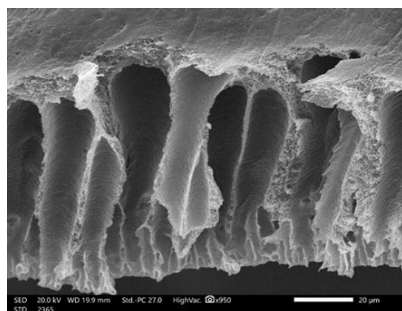


Figure 11: cross section of the composite membrane

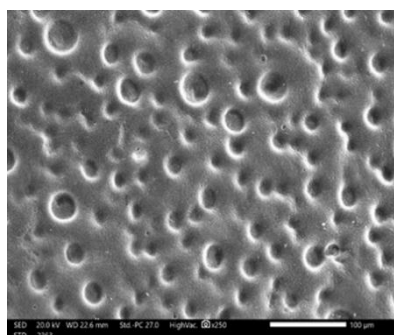


Figure 12: Micrographs of the bottom of composite membrane

3.6 X-ray diffraction (XRD)

The sample was subjected to an X-ray diffraction (XRD) investigation utilizing a Rigaku, (Model: D/B max) X-ray diffractometer with a Cu-K monochromatic radiation at a set operating voltage and current of 30 mA. At room temperature, all analyses were performed using a 2-second scan from 20 to 90 degrees. The data collecting step size was 0.05°, with a scanning rate of 1.80.min⁻¹. On a double-faced adhesive tape, the powder was equally distributed before being applied to the sample holder. After that, the holder was put inside the chamber to measure the peaks' angular distribution using X-ray diffraction (XRD). Using the Jade software, the captured patterns were compared to a comparable standard file. Early research revealed that a characteristic of a pure CS sample film is the presence of two distinct crystalline peaks at $2\theta = 15.10$ and 20.90 . According to Figure 13.a [18-19], these crystalline peaks at 15.10 and 20.90 correspond to the reflection planes of (110) and (220), respectively. The intramolecular and intermolecular hydrogen bonds, which represent an average intermolecular distance of the crystalline sections of CS, are primarily credited with maintaining the rigid crystalline structure of CS. PVA is sufficiently attached to the main chain by OH groups in order to have both strong intramolecular and intermolecular hydrogen bonds. Figure 10.b displays the XRD pattern of pure CS and PVA films. Pure PVA's semi-crystalline characteristics are demonstrated by a prominent peak at $2\theta = 180$ [20-21]. PVA is sufficiently attached to the main chain by OH groups in order to have both strong intramolecular and intermolecular hydrogen bonds. Notably, the PVA structure's amorphous phases are indicated by a significant peak center at $2\theta = 30.70$. This study shown that when CS and PVA were combined, the direction peaks' intensity and expanded. Due to the prevalence of the amorphous structure in the mix system, this results in the breaking of hydrogen bonds. Consequently, polymer blending may be regarded as a traditional approach of reducing the PVA crystalline section.

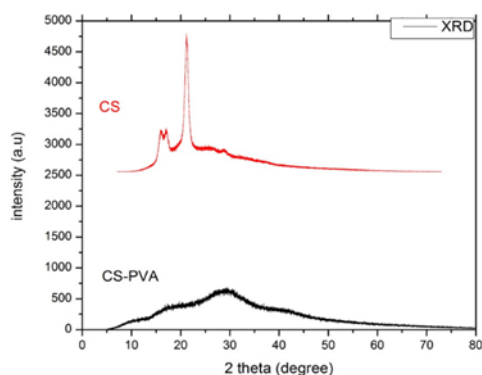


Figure 13: XRD pattern of a) CS b) CS-PVA

3.7 Removal of copper, chromium, and zinc ions by CS/PVA membrane

A 100 mL solution of three different heavy metals (copper, chromium, and zinc) was prepared with a concentration of 3 ppm in order to assess the adsorption performance of CS/PVA membrane in heavy metal removal. Atomic absorption spectroscopy was used to determine the residual concentration of the filtrate after the solution was passed through membrane. The concentration of residual copper after membrane adsorption in the case of copper ion removal is 1.8062 ppm, yielding a high removal percentage of 63.6%. After membrane adsorption, there is 1.6469 ppm of residual chromium for chromium ion removal, translating to a removal rate of 45%. The concentration of residual zinc after membrane adsorption is 1.2127 ppm, giving a percentage removal of 59.57% for the removal of zinc ions.

3.8 Removal of copper, chromium, and zinc ions by CA-RO/CS/PVA composite membrane

The same three heavy metals (copper, chromium, and zinc) utilized in the CS/PVA membrane are used to test the adsorption effectiveness of the composite membrane in heavy metal removal. Once more, the solution was passed through a membrane, and atomic absorption spectroscopy was used to determine the residual concentration of the filtrate. The concentration of residual copper after membrane adsorption in the case of copper ion removal is 0.2809 ppm, yielding a very high percentage removal of 90.5%. Since the residual concentration of the metal was 0.0471 ppm, the removal percentage for chromium ions was the highest at 98.33%. With a residual zinc ion concentration of 0.866 ppm, the percentage of zinc removed was 73.11%.

3.9 Application of CS/PVA membrane and CA-RO/CS/PVA composite in desalination

To examine both prepared membranes' capacity for desalination, A 156 g/L salt solution was made, and its conductivity was assessed both before and after membrane application. The conductivity of CS/PVA reduced to 33.1 mS after passing salt water with a conductivity of 120 mS, a conductivity loss of 72.5%. Conversely, spraying salt water onto the composite reduced the water conductivity to 20 mS, a decrease in conductivity of 83.33%.

4 CONCLUSIONS

The current study's first phase entailed extracting chitosan from mussel shells. The second phase involved electrospinning blended Chitosan-PVA fibres (CS/PVA) and studying the effect of electrical voltage on fiber diameter. The fibers produced by electrospinning are found to be in the nano range (182.2 nm-459.2 nm). The higher the voltage, the smaller the diameter of the fiber. In the third phase, two types of membranes were created: a CS/PVA membrane (50/50 %vol) and a composite membrane created by grafting PVA and Chitosan onto a CA-RO membrane (CS/PVA- CA-RO). The fourth phase involved investigating the structural details and crystallinity of the membrane using scanning electron microscopy (SEM), X-ray Powder Diffraction (XRD), and infrared spectroscopy (FTIR). In contrast to the composite membrane, which appeared uniform and smooth, SEM micrographs revealed that the surface of the CS/PVA membrane is identical to that of the fibers. A cross section of the composite membrane revealed numerous holes caused by grafting. The final stage involved the use of both fabricated membranes in heavy metal removal and desalination. The CS/PVA membrane worked well for removing copper, chromium, and zinc ions. It was also effective at removing salt. In terms of salt and heavy metal removal, the composite membrane outperformed the CS/PVA membrane.

Credit Authorship Contribution Statement

Author 1, Conceptualization, methodology, validation, investigation, resources, data curation, writing—original draft preparation, writing—review and editing.

Author 2, Writing -original draft preparation.

Author 3, Data curation, writing—original draft preparation, writing—review and editing.

Conflicts of interest

The authors declare there is no conflict of interest.

5 REFERENCES

- [1] Abdur Rehman, Seid Mahdi Jafari, Qunyi Tong, Tahreem Riaz, Elham Assadpour, Rana Muhammad Aadil, Sobia Niazi, Imran Mahmood Khan, Qayyum Shehzad, Ahmad Ali, Sohail Khan. Drug nanodelivery systems based on natural polysaccharides against different diseases. *Adv Colloid Interface Sci* 2020; 284 102251. <https://doi.org/10.1016/j.cis.2020.102251>
- [2] Abo Elsoud, M.M., El Kady, E.M. Current trends in fungal biosynthesis of chitin and chitosan. *Bull Natl Res Cent* 2019; 43, 59. <https://doi.org/10.1186/s42269-019-0105-y>.
- [3] Pokhrel, S., Yadav, P. N., & Adhikari, R. Applications of Chitin and Chitosan in Industry and Medical Science: A Review. *Nepal J Sci Technol* 2016; 16(1): 99–104. <https://doi.org/10.3126/njst.v16i1.14363>.
- [4] Mohammad Khajavian, Vahid Vatanpour , Roberto Castro-Muñoz , Grzegorz Boczkaj. Chitin and derivative chitosan-based structures — Preparation strategies aided by deep eutectic solvents: A review. *Carbohydr Polym* 2022; 275 118702. <https://doi.org/10.1016/j.carbpol.2021.118702>.
- [5] Cameron W. Irvin , Chinmay C. Satam, J. Carson Meredith , Meisha L. Shofner. Mechanical reinforcement and thermal properties of PVA tricomponent nanocomposites with chitin nanofibers and cellulose nanocrystals. *Compos Appl Sci Manuf* 2019; 116: 147-157. <https://doi.org/10.1016/j.compositesa.2018.10.028>.
- [6] K.M. Liew , M.F. Kai, L.W. Zhang. Carbon nanotube reinforced cementitious composites: an overview. *Compos. Appl Sci Manuf* 2016; 91(1):301-323. <https://doi.org/10.1016/j.compositesa.2016.10.020>.
- [7] Kozma M., Acharya B., Bissessur R. Chitin, Chitosan, and Nanochitin: Extraction, Synthesis, and Applications. *Polymers* 2022; 14(19) 3989. <https://doi.org/10.3390/polym14193989>.
- [8] Wu, Y.; Rashidpour, A.; Almajano, M.P.; Metón, I. Chitosan-Based Drug Delivery System: Applications in Fish Biotechnology. *Polymers* 2020; 12(5): 1177. <https://doi.org/10.3390/polym12051177>.
- [9] Shameem Hasan, Veera M. Boddu, Dabir S. Viswanath, Tushar K. Ghosh. Chitin and Chitosan Science and Engineering. Switzerland: Engineering Materials and Processes, Springer Nature; 2022. <https://doi.org/10.1007/978-3-031-01229-7>.
- [10] Vishnu Bhaskar, Sriramani Mangipudi, Mohammed Rivin S, Talloju Karanam Hemanth Kumar, Noel Jacob Kaleekkal. Electrospun nanofibrous membranes for membrane distillation. *Nano-Enabled Technologies for Water Remediation Micro and Nano Technologies* 2022; 215-261. <https://doi.org/10.1016/B978-0-323-85445-0.00014-X>.
- [11] Natalia Fijo, Andrea Aguilar-Sánchez Aji P. Mathew, 3D-printable biopolymer-based materials for water treatment: A review. *Chem Eng J* 2022; 430(3). <https://doi.org/10.1016/j.cej.2021.132964>.
- [12] Ehsan Salehia, Mohammad Khajavian. Advances in nanocomposite and nanostructured chitosan membrane adsorbents for environmental remediation: A review. *Desalination* 2022; 527. <https://doi.org/10.1016/j.desal.2022.115565>.
- [13] Yudin, V. E., Dobrovolskaya, I. P., Neelov, I. M., Dresvyanina, E. N., Popryadukhin, P. V., Ivan'Kova, E. M., Morganti, P. Wet spinning of fibers made of chitosan and chitin nanofibrils. *Carbohydrate Polymers* 2014; 108(1): 176–182. <https://doi.org/10.1016/j.carbpol.2014.02.090>.
- [14] Vega-Cázarez, Claudia A. ; López-Cervantes, Jaime ; Sánchez-Machado, Dalia I. ; Madera-Santana, Tomás J. ; Soto-Cota, Adolfo ; Ramírez-Wong, Benjamín. Preparation and Properties of Chitosan–PVA Fibers Produced by Wet Spinning. *J Polym Environ* 2018; 946-958.
- [15] Ugwu, E.I., Agunwamba, J.C. A review on the applicability of activated carbon derived from plant biomass in adsorption of chromium, copper, and zinc from industrial wastewater. *Environ Monit Assess* 2020; 192: 240 . <https://doi.org/10.1007/s10661-020-8162-0>.
- [16] Basma Al-Najara; Christian D. Peters. Pressure and osmotically driven membrane processes: A review of the benefits and production of nano-enhanced membranes for desalination. *Desalination* 2020; 479. <https://doi.org/10.1016/j.desal.2020.114323>.

[17] Hyeon Ung Shin, Yalong Li, Ariel Paynter, Kitchaporn Nartetamrongsutt, and George G. Chase. Microscopy analysis and production rate data for needleless vertical rods electrospinning parameters. Data in Brief 2015; 5:41-44. [http://doi: 10.1016/j.dib.2015.08.005](http://doi:10.1016/j.dib.2015.08.005).

[18] S. Zargham, S. Bazgir, A. Tavakoli, A. S. Rashidi, and R. Damerchely. The Effect of Flow Rate on Morphology and Deposition Area of Electrospun Nylon 6 Nanofiber. J. Eng. Fiber. Fabr 2012;7(4). <https://doi.org/10.1177/1558925012007004>.

[19] S. Haider, W.A. Al-Masry, N. Bukhari, M. Javid. Thermoplastic Nanocomposites and Their Processing Techniques. Polym Eng Sci 2010; 50 (1): 120-127.

[20] Shujahadeen B. Aziz, Shakhawan Al-Zangana, M. A. Brza, Salah Raza Saeed, Rebar T. Abdulwahid, M. F. Z. Kadir. Study of Dielectric Properties and Ion Transport Parameters in Chitosan-Barium Nitrate Based Solid Polymer Electrolytes. Int. J. Electrochem. Sci. 2019; 14:11580–11595. [http://doi: 10.20964/2019.12.39](http://doi:10.20964/2019.12.39).

[21] Aziz, S.B. Role of Dielectric Constant on Ion Transport: Reformulated Arrhenius Equation. Adv. Mater. Sci. Eng. 2016; 1-12. <https://doi.org/10.1155/2016/2527013>.